Magnetic Resonance Studies on the Active Site and Metal Centers of *Bradyrhizobium japonicum* Porphobilinogen Synthase†

Robert M. Petrovich and Eileen K. Jaffe*

Institute for Cancer Research, Fox Chase Cancer Center, 7701 Burholme Avenue, Philadelphia, Pennsylvania 19111

Received July 8, 1997⊗

ABSTRACT: Porphobilinogen synthase (PBGS) is a metalloenzyme which catalyzes the asymmetric condensation of two molecules of 5-aminolevulinic acid (ALA) to form porphobilinogen. There are at least four types of PBGS, categorized according to metal ion usage. The PBGS from *Bradyrhizobium japonicum* requires Mg(II) in catalytic metal site A, has an allosteric Mg(II) in metal site C, and also contains an activating monovalent cation binding site [Petrovich et al. (1996) *J. Biol. Chem. 271,* 8692−8699]. ^{13}C NMR and Mn(II) EPR have been used to probe the active site and Mg(II) binding sites of this 310 000 dalton protein. The ^{13}C NMR chemical shifts of enzyme-bound product demonstrate that the chemical environment of porphobilinogen bound to *B. japonicum* PBGS is different from that of PBGS which contains Zn(II) rather than Mg(II) at the active site. Use of Mn(II) in place of Mg(II) broadens the NMR resonances of enzyme-bound porphobilinogen, providing evidence for a direct interaction between Mn_A and product at the active site. Prior characterization of the enzyme defined conditions in which the divalent cation occupies either the A or the C site. Mimicking these conditions allows Mn(II) EPR observation of either Mn_C or Mn_A. The EPR spectrum of Mn_C is significantly broader and less intense than "free" Mn(II), but relatively featureless. The EPR spectrum of Mn_A is broader still and more asymmetric than Mn_C. The EPR data indicate that the coordination spheres of the two metals are different.

Porphobilinogen synthase (PBGS,[1] *a.k.a.* 5-aminolevulinate dehydratase, EC 4.2.1.24) is the first enzyme shown to have experienced a phylogenetic shift between a catalytic Zn(II) and a catalytic Mg(II). PBGS catalyzes the asymmetric condensation of two molecules of 5-aminolevulinate (ALA) to form porphobilinogen, the monopyrrole precursor of the porphyrins, chlorophylls, corrins, and cofactor F430 (see Figure 1). The phylogenetic variations in divalent metal ion usage of PBGS can be described in terms of three different types of divalent binding sites called A, B, and C (*1*). The function of the divalent ion in site A is to facilitate A-side ALA binding and reactivity (see ref *1* and Figure 1). Although the B-site metal ion has been proposed to aid in the removal of a proton lost during porphobilinogen formation, it has not been found to be "essential" (*2*). Based on studies of mammalian PBGS, four A-site metal ions and four B-site metal ions bind to each octamer (*1*, *3*, *4*), equivalent to the stoichiometry of four active sites. To help explain the stoichiometry of metal sites A and B, a putative metal binding domain of each subunit has been proposed to provide ligands to *either* the A-site or the B-site metal ions (*3*, *4*). The C-site metal ion, which binds elsewhere in the sequence, is an allosteric activator that increases the V_{max}, decreases the K_m for ALA, and decreases the K_d for metal ions in sites A and B; its stoichiometry is 8 per octamer (*5*, *6*). Table 1 summarizes this model for divalent metal ion interactions with PBGS; by the criteria set out in Table 1, there are at least four types of PBGS. In addition, some PBGS respond to monovalent cations (*7*, *8*, *9*). Despite the differences in metal ion usage, a universally conserved lysine that forms a Schiff base with one ALA and high overall sequence conservation suggest that all PBGS's use a common catalytic mechanism.

The plant endosymbiot *Bradyrhizobium japonicum* produces a Mg-utilizing type IV PBGS (*B. japonicum* PBGS) protein (see Table 1) which also responds to monovalent cations (*9*). We have undertaken ^{13}C NMR and Mn(II) EPR studies of *B. japonicum* PBGS to probe its active site and metal binding sites. The results of these studies are compared to our previous studies of types I and II PBGS (*5*, *6*, *10*, *11*, *12*). The comparison is consistent with a model where type IV PBGS uses a catalytic Mg_A while types I and II PBGS use a catalytic Zn_A. These results are inconsistent with an alternative model in which type II PBGS uses eight catalytic Mg_α and eight allosteric Zn_β (*13*, *14*, *15*).

MATERIALS AND METHODS

Materials. The chemicals KCl, potassium phosphate, phenylmethylsulfonyl fluoride, ampicillin, chloramphenicol, TES, trichloroacetic acid, *p*-(dimethylamino)benzaldehyde, dithiothreitol, ALA, isopropyl β-D-thiogalactopyranoside, bis-tris propane, EDTA (free acid), D_2O (99.9%), and DCl (100%) were all purchased from Sigma, and are ACS reagent grade or better. KOH was purchased from Aldrich. Ultrapure $MgCl_2$ was purchased from Johnson Matthey. Glacial acetic acid and 70% perchloric acid were purchased from Fisher and are ACS reagent grade. 2-Mercaptoethanol was purchased from Fluka and vacuum-distilled prior to use.

† This research was supported by NIH Grants ES03654 (E.K.J.), CA09035, and CA06927 (Institute for Cancer Research), and by an appropriation from the Commonwealth of Pennsylvania.

* To whom correspondence should be addressed. Telephone: 215-728-3695. Fax: 215-728-2412. E-mail: EK_Jaffe@fccc.edu.

⊗ Abstract published in *Advance ACS Abstracts,* October 15, 1997.

[1] Abbreviations: PBGS, porphobilinogen synthase; ALA, 5-aminolevulinic acid; TES, *N*-[tris(hydroxymethyl)methyl]-2-aminoethanesulfonic acid; bis-tris propane, 1,3-bis[tris(hydroxymethyl)methylamino]-propane; NMR, nuclear magnetic resonance; EPR, electron paramagnetic resonance; EDTA, ethylenediaminetetraacetic acid.

S0006-2960(97)01642-5 CCC: $14.00 © 1997 American Chemical Society

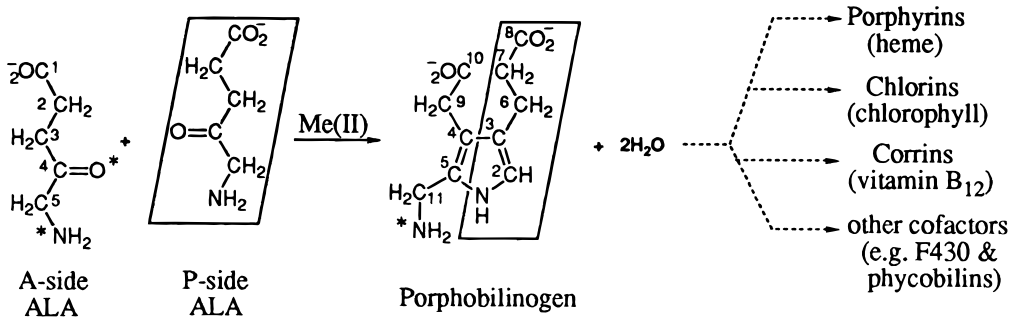

FIGURE 1: PBGS-catalyzed reaction. A-side ALA becomes the *a*cetyl-containing half of porphobilinogen and retains the primary *a*mino group. P-side ALA becomes the *p*ropionyl-containing half of porphobilinogen; its amino group is incorporated into the *p*yrrole ring. The asterisks reflect the probable substrate- or product-derived ligands to the catalytic A-site metal ion.

Table 1: Three Divalent Metal Ion Model for PBGS

		metal ion required for full activity per homooctamer		
type	example	site A	site B	site C
I	mammal[a]	4 Zn(II)	4 Zn(II)[b]	absent
II	*E. coli*[c,d]	4 Zn(II)	4 Zn(II)	8 Mg(II)
III	plant[e]	4 Mg(II)	4 Mg(II)	8 Mg(II)
IV	*B. japonicum*[f]	4 Mg(II)	absent	8 Mg(II)

[a] Refs *3*, *21*. [b] Not strictly required (ref 2). [c] Refs *5*, *6*. [d] Total stoichiometry according to ref *13*. [e] Total stoichiometry according to ref *22*. [f] Ref *9*.

Ultrapure ammonium sulfate was purchased from ICN Biomedical. Phenyl-Sepharose and Sephacryl S-300 high-resolution matrixes were purchased from Pharmacia. [4-^{13}C]-ALA, [5-^{13}C]ALA, and [3-^{13}C]ALA were custom-synthesized by C/D/N Isotopes. DEAE-biogel A gel was purchased from BioRad. Centricon-10 concentration devices were purchased from Amicon. Slide-A-Lyser cassettes were purchased from Pierce.

[5-^{13}C]ALA was deuterated at C_3 and C_5 as previously described with minor modification (*11*). A solution of 0.1 M [5-^{13}C]ALA-HCl and 0.1 M bis-tris propane, in 99.9% D_2O, was adjusted to pH 7.1 (meter reading) with DCl and incubated in a flame-sealed vial for 48 h at 37 °C. The use of bis-tris propane rather than potassium phosphate caused a slower exchange rate at C_5, and no self-condensation was observed. The resultant [5-^{13}C]ALA was ~98% deuterated at C_5 as determined by ^{13}C NMR.

PBGS Purification. B. japonicum PBGS was expressed in *E. coli* and purified as previously reported (*9*) with the following modification. The final step in the protein purification was passage through a 5 × 100 cm Sephacryl S-300 high-resolution column in 0.1 M KP_i, pH 7.0, containing 1 mM $MgCl_2$. This column removes the mercaptoethanol and separates PBGS from a contaminating activity which degrades porphobilinogen. *B. japonicum* PBGS elutes at ~1050 mL.

Preparation of Metal-Free Apo-Enzyme. Apo-*B. japonicum* PBGS was prepared by dialyzing 1−3 mL of concentrated enzyme (35−150 mg/mL) in a Slide-A-Lyser cassette for 6 h against l L of 50 mM bis-tris propane-HCl buffer, pH 7.0, followed by an overnight dialysis against a second liter of the same buffer. After dialysis, the protein was concentrated using a Centricon-10 device. Apo-enzyme was always prepared just prior to use, as apo-enzyme is relatively unstable and slowly loses activity even when stored at 4 °C. Apo-enzyme is inactive and requires addition of Mg(II) for activity.

PBGS Activity Assays. Activity assays were carried out as previously described with the exception that 2-mercaptoethanol was omitted from the assay and mercuric chloride was omitted from the STOP reagent (*9*). The activity as a function of Mg(II) *vs* Mn(II) studies were performed using apo-enzyme and 0.1 M TES−KOH, pH 8.2, buffer. Enzyme concentration was held constant at 0.9 μM. The addition of ALA under these conditions causes the final pH of the assays to be 8.0. Specific activity is expressed as micromoles of porphobilinogen produced per milligram of protein per hour at 37 °C.

^{13}C NMR Studies. ^{13}C NMR spectra were obtained at 75.45 MHz on a Bruker AM300 spectrometer by using acquisition parameters identical with those reported previously for studies of porphobilinogen bound to bovine PBGS (*10*, *11*, *12*). Spectra were acquired with a 45° pulse and a 2 s repetition rate and were digitized at a resolution of 1.2 Hz/point. Spectra were obtained at 37 °C, unless otherwise indicated. Protein spectra were processed with a 15 Hz Lorentzian line-broadening function. Proton decoupling was achieved using a Waltz-16 pulse sequence.

Mn(II) EPR Studies. X-band (9.14 GHz) EPR spectra were obtained on a computer-interfaced Varian E-109 spectrometer. Binding studies were performed at 25 °C; single scans were recorded with the spectrometer settings of 1 mW microwave power, 10 G modulation amplitude, a sweep rate of 4.17 G/s, and a time constant of 0.128 s. The receiver gain was varied from 1.25×10^3 to 1.6×10^4 depending on signal intensity. Spectra of enzyme-bound Mn(II) were recorded at 10 mW microwave power and are an average of 4 scans.

The EPR samples were all prepared from apo-*B. japonicum* PBGS. Because a reaction was observed between Mn(II) and bis-tris propane, prior to EPR studies the apo-enzyme was dialyzed against 2 L of 0.1 M TES−KOH, pH 8.2, for 16 h. Samples of *B. japonicum* PBGS plus Mn(II) were prepared by mixing 40 μL of apo-*B. japonicum* PBGS (45 mg/mL) with 10 μL of a Mn(II) solution in 0.1 M TES−KOH, pH 8.2. The final concentration of Mn(II) ranged from 0 to 2 mM. Samples of *B. japonicum* PBGS plus Mn(II) in the presence of porphobilinogen were prepared by mixing 25 μL of 74 mg/mL apo-*B. japonicum* PBGS in 0.1 M TES−KOH, pH 8.2, with 10 μL of Mn(II) solution in 0.1 M TES−KOH, pH 8.2, and 15 μL of 14 mM ALA in 0.1 M TES−KOH, pH 8.2. The final concentration of Mn(II) ranged from 0 to 4 mM. The samples were allowed to react for ≥10 min prior to scanning to allow full conversion of ALA to porphobilinogen.

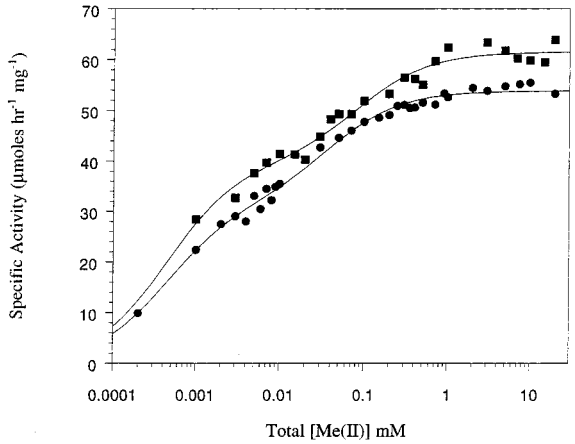

FIGURE 2: Comparison of the effect of Mg(II) (●) or Mn(II) (■) on *B. japonicum* PBGS activity in 0.1 M TES−KOH at pH 8.2 demonstrates that Mn(II) can be used as a valid probe for the Mg(II) of *B. japonicum* PBGS. The lines were generated using a two-independent site model (9) expressed in eq 1, and the best-fit results are included in Table 2.

RESULTS

Prior characterization of *B. japonicum* PBGS revealed that the substrate and divalent metal binding properties are dependent upon each other as well as being dependent upon pH and monovalent cations (*9*). Based on these results and the model presented in Table 1, one can capitalize upon these characteristics to prepare NMR and EPR samples under a variety of conditions such that the protein will differ in its propensity to bind product, Mn_A, and/or Mn_C. The NMR and EPR studies described here were employed to test the model which derived from our interpretation of kinetic and metal binding data (*9*).

Activity as a Function of Mn(II). In order to use Mn(II) as a paramagnetic EPR probe for the Mg(II) of *B. japonicum* PBGS, one must first demonstrate that Mn(II) functionally substitutes for Mg(II). Because the buffer previously used to characterize the interaction of Mg(II) with *B. japonicum* PBGS (*9*) was found to react with Mn(II), we used the buffer TES−KOH for a kinetic comparison of the effects of Mg(II) and Mn(II) on *B. japonicum* PBGS and for all experiments where excess Mn(II) was used.

The dependence of *B. japonicum* PBGS activity on added Mg(II) or Mn(II) at pH 8.2 in 0.1 M TES−KOH are compared in Figure 2. The simplest model to fit the sets of data is a two-site model, where the tight binding metal ion is essential for activity (Me_A) and the second looser binding metal ion acts as an allosteric activator (Me_C). This model is also valid for Mg(II) in bis-tris propane if K^+ is present to satisfy the monovalent cation requirement (*9*). The lines in Figure 2 were generated by eq 1 using the best-fit values in Table 2; where $K_{d(req)}$ is the dissociation constant for the essential metal ion, V_0 is the maximal activity in the absence of the allosteric metal ion, $K_{d(act)}$ is the dissociation constant for the allosteric metal ion, and the activation factor is the fold activation upon binding the allosteric metal ion.

$$\text{specific activity} = \frac{V_0[\text{Me(II)}]}{K_{d(req)} + [\text{Me(II)}]} + \frac{[(V_0 \times \text{activation factor}) - V_0][\text{Me(II)}]}{K_{d(act)} + [\text{Me(II)}]} \quad (1)$$

Table 2: Kinetic Parameters for the Mg(II)- or Mn(II)-Dependent Activity of *B. japonicum* PBGS at pH 8.2

metal	buffer	$K_{d(req)}$[a] (μM)	V_0	$K_{d(act)}$[b] (μM)	activation factor	V_{max} (μmol h^{-1} mg^{-1})
Mg(II)[c]	bis-tris propane + KCl	≤0.3	22 ± 1	39 ± 7	2.0	44.4
Mg(II)	TES−KOH	≤0.4	31 ± 1	37 ± 6	1.7	53.9
Mn(II)	TES−KOH	≤0.4	39 ± 2	83 ± 22	1.6	61.5

[a] This reflects the K_d for the A-site metal in the presence of substrate or product. [b] This reflects the K_d for the C-site metal in the presence of substrate or product. [c] Ref 9.

The value of $K_{d(req)}$ for both Mg(II) and Mn(II) is an upper limit because these assays used *B. japonicum* PBGS at ∼1 μM subunits; thus, total Me(II) is a poor approximation for free [Me(II)] at [Me(II)] below 5 μM. V_0 is slightly higher for Mn(II) than for Mg(II). The activation factors for the two metal ions are virtually identical. However, the $K_{d(act)}$ for Mn(II) is roughly twice that of Mg(II). Table 2 shows that the kinetic values are all very similar to those previously reported for Mg(II) in bis-tris propane at pH 8.2 in the presence of K^+ (conditions where the K_d for K^+ ≤1 mM; ref 9). This kinetic model was shown to be invalid in the absence of K^+. Without K^+, the response of specific activity to Mg(II) is cooperative with a Hill coefficient of ∼2 (see ref *9*).

Mn(II) EPR of Me_A and Me_C Bound to B. japonicum PBGS. *B. japonicum* PBGS preferentially binds Me_C over Me_A in the absence of substrate or product and Me_A over Me_C in the presence of substrate or product (ref *9* and Table 2). This is confirmed by the spectra illustrated in Figure 3. The EPR spectrum of "free" Mn(II) in TES−KOH is illustrated in Figure 3A. One can achieve specific binding of Mn(II) to the C-sites (K_d 80−160 μM, capacity 2/active site) *vs* the A-sites ($K_d \geq 1$ mM, capacity 1/active site) at millimolar concentrations of *B. japonicum* PBGS active sites (dimers) by using a substoichiometric amount of Mn(II) in the absence of substrate or product. The addition of 0.5 mM Mn(II) to 1.1 mM *B. japonicum* PBGS active sites at pH 8 yields the spectrum illustrated in Figure 3B. The lines are modestly broadened relative to "free" Mn(II), and the intensity is reduced by a factor of ∼10. The [Mn(II)] "free" under these conditions is calculated to be between 0.02 and 0.04 mM. Due to the intensity differences between "free" and bound Mn(II), even these relatively low amounts of "free" Mn(II) contribute appreciably to the Mn(II) EPR spectrum. Figure 3C is the result of subtracting 4.8% of Figure 3A from Figure 3B, and is a more accurate representation of the EPR spectrum of Mn_C bound to *B. japonicum* PBGS. At subsaturating Mn(II), the addition of substrate is predicted to cause a migration of Mn_C to Mn_A. In fact, the addition of excess ALA (∼4 mM) causes a dramatic change in the Mn(II) EPR spectrum as illustrated in Figure 3D. The line shape becomes distinctly asymmetric, and the intensity decreases by another factor of 2. According to the kinetic data in Table 2, the distribution of Mn(II) is now calculated to be 98% Mn_A, 2% Mn_C, and <0.1% "free" Mn(II). At these concentrations, neither "free" Mn(II) nor Mn_C is expected to contribute appreciably to the spectrum in Figure 3D. Thus, the Mn(II) EPR spectra demonstrate the predicted disproportionation of Mn(II) from the C-sites to the A-sites upon the addition of substrate or product.

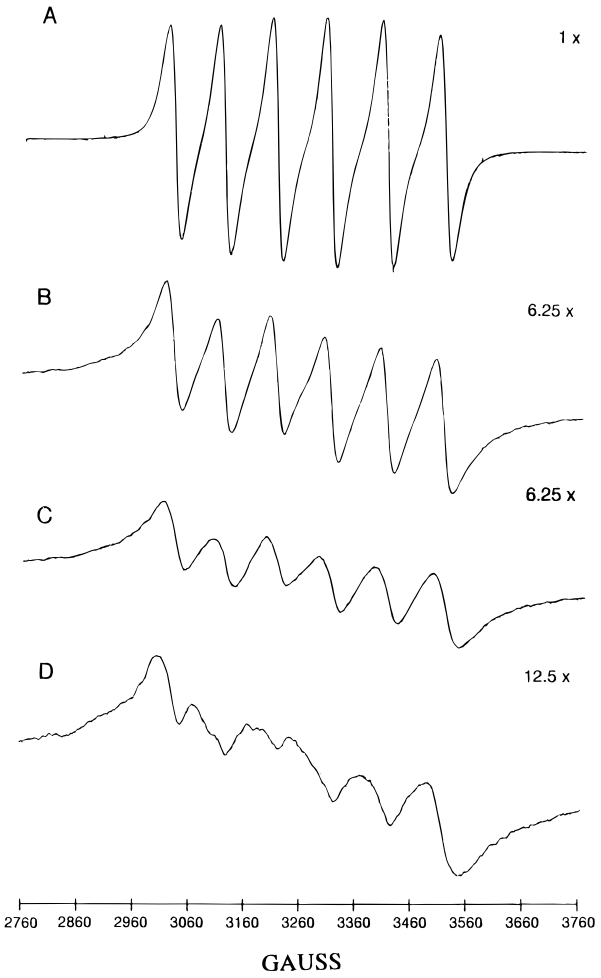

FIGURE 3: Mn(II) EPR spectra. (A) 0.5 mM Mn(II) in 0.1 M TES−KOH, pH 8.2. This spectrum represents "free" Mn(II). (B) Sample A plus 1.1 mM *B. japonicum* PBGS active sites. Under these conditions, Mn(II) is primarily at the Me_C sites with some remaining free. (C) Spectrum B minus 4.8% of spectrum A to correct for the free component in spectrum B. (D) Sample B plus 2 mM porphobilinogen. Addition of product causes disproportionation of Mn(II) from the Me_C sites to the Me_A sites. Porphobilinogen is proposed to be directly bound to the catalytic A-site metal ion (1).

Mn(II) Binding Stoichiometry by EPR. The high intensity of the EPR signals for Mn(II) bound to *B. japonicum* PBGS at either the A-sites or the C-sites precludes the use of a standard Scatchard type analysis to determine Mn(II) stoichiometries and affinities, because the intensity of the bound Mn(II) signal is not negligible compared to that of "free" Mn(II) (*16*). Therefore, the stoichiometry of bound Mn(II) was determined by modeling binding curves generated by plotting the EPR signal intensity as a function of Mn(II) concentration in the presence of ~1 mM *B. japonicum* PBGS subunits in both the presence and absence of porphobilinogen (Figure 4). In the presence of porphobilinogen, the predominant signal seen at low [Mn(II)], less than 0.6 Mn(II)/subunit, is that of Mn_A (Figure 3D). The addition of more Mn(II) is followed by the appearance and then dominance of the Mn_C signal (Figure 3C). Addition of Mn(II) above 1.6/subunit results in the appearance and then dominance of the "free" Mn(II) signal (Figure 3A). In the absence of porphobilinogen, one observes Me(II) association with enzyme alone rather than with the enzyme·product complex. Under these conditions, the predominant signal seen at low [Mn(II)] is that of the Mn_C (Figure 3C) which, upon addition

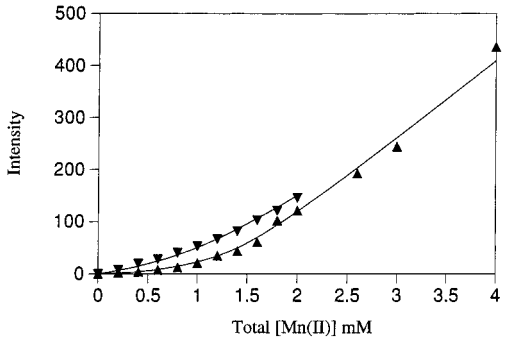

FIGURE 4: EPR signal intensity of Mn(II) plus *B. japonicum* PBGS in the presence (▲) and absence (▼) of porphobilinogen. The concentration of *B. japonicum* PBGS subunits was 0.96 mM in the presence of porphobilinogen and 0.93 mM in the absence of porphobilinogen. The lines where generated by summing the intensity contributions of Mn_A, Mn_C, and free Mn(II) as calculated using K_{d_A} = 0.4 μM and K_{d_C} = 83 μM in the presence of porphobilinogen and K_{d_A} = 1 mM and K_{d_C} = 120 μM in the absence of porphobilinogen. In both cases, the intensity of the EPR signal from Mn_A is 10 arbitrary units, Mn_C is 17−20 arbitrary units, and free Mn(II) is 140−150 arbitrary units.

of more Mn(II), gradually changes to the signal for free Mn(II) (Figure 3A). This is in keeping with our model for two types of Mn(II) binding sites with four Mn(II) at the A-site and eight Mn(II) at the C-site per homooctamer (*9*). The lines in Figure 4 were generated using eq 2:

$$I_t = I_f X_f + I_a X_a + I_c X_c \quad (2)$$

where I_t is the observed intensity of the Mn(II) EPR signal; I_f, I_a, and I_c are the intensities for the EPR signal for 1 mM Mn(II) "free" in solution, bound in site A, and bound in site C, respectively; and X_f, X_a, and X_c are millimolar concentrations of "free" Mn(II), Mn(II) bound in site A, and Mn(II) bound in site C, respectively. The best-fit lines shown in Figure 4 were obtained by setting the stoichiometry for site A to 0.5 per subunit and for site C to 1 per subunit. In the presence of porphobilinogen, X_f, X_a, and X_c were determined using a K_d for site A of 0.4 μM and for site C of 83 μM. In the presence of porphobilinogen, the best-fit values used for I_f, I_a, and I_c were 150, 10, and 17. In the absence of porphobilinogen, X_f, X_a, and X_c were determined using a K_d for site A of 1 mM and for site C of 120 μM. In the absence of porphobilinogen, the values used for I_f, I_a, and I_c were 140, 10, and 20. The K_d values used for the linear fits were derived from the experimentally determined values for both Mn(II) in the presence of porphobilinogen and Mg(II) in the presence and absence of porphobilinogen (*9*).

^{13}C NMR Studies of Product Bound to PBGS. In order to probe the active site environment, the chemical shifts and line widths of enzyme-bound ^{13}C-labeled porphobilinogen have been determined for *B. japonicum* PBGS using ^{13}C labels at all of the carbons which participate in bond-making or bond-breaking events during the PBGS-catalyzed reaction (see Table 3). Isotopically-enriched [3-^{13}C]ALA, [4-^{13}C]-ALA, and [5-^{13}C]ALA, when used individually as substrates, yield the products [4,6-^{13}C]porphobilinogen, [3,5-^{13}C]porphobilinogen, and [2,11-^{13}C]porphobilinogen, respectively (see Figure 1). The quaternary carbons C_3, C_4, and C_5 of porphobilinogen can yield relatively sharp lines when bound to a 310 000 dalton protein, so long as the temperature of data acquisition is mildly elevated (37 °C), because they have no directly attached protons which can cause severe dipolar

Table 3: ^{13}C NMR Parameters of Porphobilinogen both Free and Bound to Various PBGS

	chemical shift, δ (ppm)		chemical shift differences between free and bound porphobilinogen, $\Delta\delta$ (ppm)		
carbon	free	bound to *B. japonicum* PBGS	*B. japonicum* PBGS	bovine[a]	*E. coli*[b]
2	116.4	114.5	−1.9	−2.8	
3	123.0	122.6	−0.4	−1.5	−1.5
4	117.9	117.3	−0.6	−3.4	
5	121.0	121.8	+0.8	+6.2	+6.2
6	21.8	nd[c]	nd[c]	0	
11	34.9	34.0	−0.9	+2.6	

[a] See refs *10, 11, 12*. [b] See ref *5*. [c] C_6 is not visible in enzyme-bound spectrum because C_6 was not deuterated.

broadening (see refs *10, 11*). As an example, Figure 5A illustrates part of the natural-abundance ^{13}C NMR spectrum of *B. japonicum* PBGS, and Figure 5B illustrates the analogous spectrum showing distinct resonances from enzyme-bound [3,5-^{13}C]porphobilinogen. However, on such a large protein, resonances from the proton-bearing ^{13}C atoms of porphobilinogen, C_2, C_6, and C_{11}, are broadened beyond observability unless said protons are replaced with deuterons (*11*). To allow observation of the methine carbon C_2 and the methylene carbon C_{11}, [5-^{13}C]ALA was deuterated through enolization in D_2O. [3-^{13}C]ALA was not deuterated since the aromatic C_4 contains no protons; thus, the methylene carbon C_6 of enzyme-bound [4,6-^{13}C]porphobilinogen remained unobservable. The chemical shifts of C_2, C_3, C_4, C_5, and C_{11} of enzyme-bound porphobilinogen are tabulated in Table 3 along with the chemical shifts from free porphobilinogen. These values are compared to those of porphobilinogen bound to bovine and *E. coli* PBGS in Table 3. The chemical shifts of free porphobilinogen are insensitive to pH in the range of 6.0−8.4. "Free" porphobilinogen does not appear in the NMR spectrum until the stoichiometry exceeds 4 porphobilinogens per octamer, consistent with 4 functional active sites per octamer, as is observed with bovine and *E. coli* PBGS (spectra not shown) (*1, 2*).

Addition of [5,5-^{2}H; 5-^{13}C]ALA to PBGS is expected to yield [2,11,11-^{2}H; 2,11-^{13}C]porphobilinogen. The ^{13}C NMR spectra of [2,11,11-^{2}H; 2,11-^{13}C]porphobilinogen bound to *B. japonicum* PBGS yielded chemical shifts of 114.5 ppm for C_2 and 34.0 ppm for C_{11} (spectra not shown). The line width of the C_2 signal was 55 Hz, consistent with there being a deuterium attached to C_2 of porphobilinogen. However, the line width for the C_{11} signal was 152 Hz, indicating an unexpected proton exchange at C_5 of A-side ALA leading to the presence of at least one proton at C_{11} in the porphobilinogen product.

Assignment of signals for the enzyme-bound species is essential for data interpretation and could be unambiguously based on hybridization except for [3,5-^{13}C]porphobilinogen. To assign the 121.8 and 122.6 ppm peaks to either C_3 or C_5, porphobilinogen was prepared using a 50:50 mix of [4-^{13}C]-ALA and [3-^{13}C]ALA. This reaction produced equal amounts of [3,5-^{13}C]porphobilinogen, [3,4-^{13}C]porphobilinogen, [5,6-^{13}C]porphobilinogen, and [4,6-^{13}C]porphobilinogen as shown in Figure 6A. The ^{13}C NMR spectrum of the porphobilinogen mixture "free" in solution is shown in Figure 6D. The signal for C_3 appears as a 1:2:1 triplet; however, it is composed of two independent signals both centered at 123.0 ppm. One signal arises from [3,5-^{13}C]porphobilinogen. This is the center resonance where J_{CC} is 3.5 Hz, and is not seen as a doublet due to the line width of the signal (*10*). The second doublet arises from [3,4-^{13}C]porphobilinogen, where J_{CC} = 53 Hz. This same pattern is observed for the C_4 resonance at 117.9 ppm where J_{CC} of [4,6-^{13}C]porphobilinogen is an unseen J coupling of ∼2 Hz and J_{CC} of [3,4-^{13}C]porphobilinogen is again 53 Hz. The singlet at 121 ppm is comprised of two superimposed unresolved doublets arising from C_5 of [3,5-^{13}C]porphobilinogen and [5,6-^{13}C]-porphobilinogen. The ^{13}C NMR spectrum of the porphobilinogen mixture bound to *B. japonicum* PBGS is shown in Figure 6B. The spectrum acquired at 37 °C (Figure 6B) looks very similar to that of [3,5-^{13}C]porphobilinogen-bound *B. japonicum* PBGS (Figure 5B), except for the new signal at 117.3 ppm due to C_4 of [3,4-^{13}C]porphobilinogen and [4,6-^{13}C]porphobilinogen. J_{C3-C4} is not observed because the inherent line width of the bound porphobilinogen is greater than the expected 53 Hz coupling. To decrease the line width, the temperature was raised in increments of 5 °C until the line width of the signal at 121.8 ppm was less than 50 Hz. If this signal derives from C_3, it should be possible to observe the C_3-C_4 coupling. Since the signal at 121.8 ppm remains a sharp "singlet", we assign this resonance to C_5. Consequently, the enzyme-bound signal at 122.6 ppm is assigned to C_3.

Having assigned the ^{13}C NMR spectra of ^{13}C-labeled porphobilinogen bound to *B. japonicum* PBGS, comparison with previous studies shows substantially different chemical shifts are observed relative to those seen for bovine or *E. coli* PBGS (*5, 12*). Prior ^{13}C and ^{15}N NMR studies of bovine and *E. coli* PBGS with [3,5-^{13}C]porphobilinogen suggest that the chemical environments of the active sites of these two enzymes are very similar if not identical to each other. For all labeled porphobilinogens, the magnitude and direction of the chemical shift changes are consistent with a dramatic elevation of the apparent active site pH *vs* that of the buffer, and support an active site model in which porphobilinogen is directly bound to a Zn(II) through a deprotonated amino group (*5, 12*). The very different chemical shifts seen for porphobilinogen bound to *B. japonicum* PBGS indicate that the chemical environment of the active site of *B. japonicum* PBGS is dramatically different than those of bovine and *E. coli* PBGS. We believe this difference is due to the active site Mg_A. Nevertheless, the absolute shifts from "free" seen with porphobilinogen bound to *B. japonicum* PBGS are again consistent with an elevation in the apparent active site pH *vs* buffer pH. The data suggest a lower active site pH for *B. japonicum* PBGS than either bovine or *E. coli* PBGS. One possible explanation is the presence of Mg(II) *vs* Zn(II) in the active site. Alternatively, the proposed ligands for the active site Mg(II) of *B. japonicum* PBGS are more acidic than those for the Zn(II) in the active site of either bovine or *E. coli* PBGS (*17*).

Effect of Mn(II) and EDTA on the ^{13}C NMR Spectrum of Enzyme-Bound [3,5-^{13}C]Porphobilinogen. Addition of [4-^{13}C]-ALA to *B. japonicum* PBGS at ∼1 mM active sites yields the spectrum illustrated in Figure 5B. When [4-^{13}C]ALA was added in excess of two per active site, free porphobilinogen was observed. The protein used to obtain the spectrum in Figure 5B was dialyzed to prepare apo-protein; then Mn(II) was added at a stoichiometry of 1/subunit along with [4-^{13}C]ALA at 1/subunit. The NMR spectrum at 1

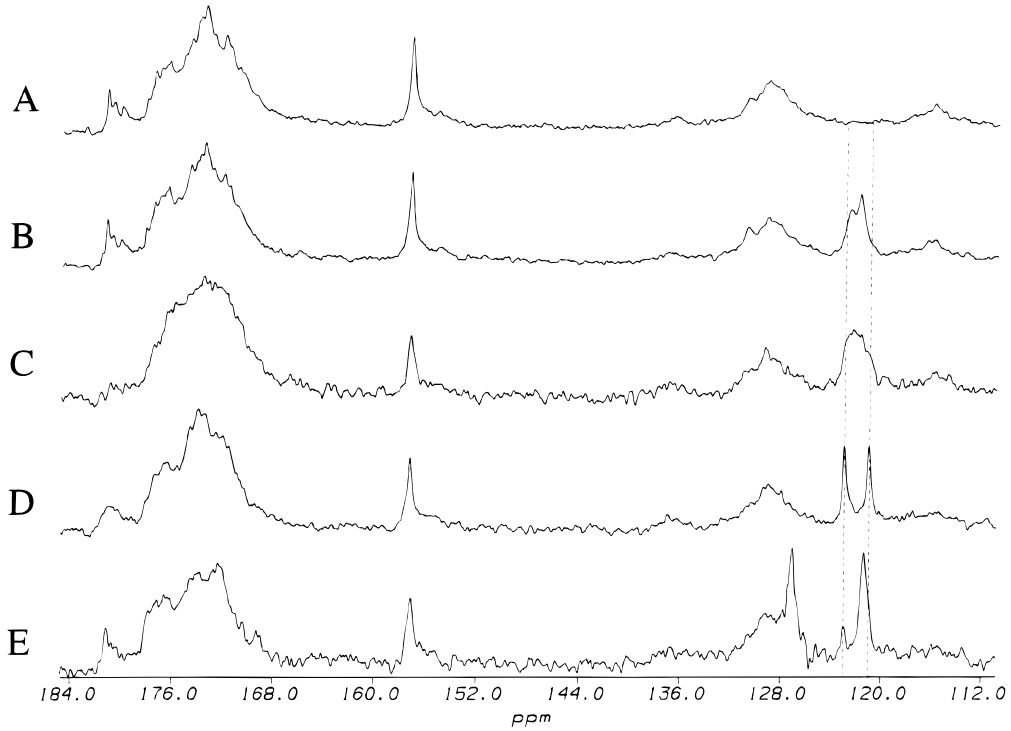

FIGURE 5: The sp and sp^2 regions of the ^{13}C NMR spectra of [3,5-^{13}C]porphobilinogen and PBGS complexes. (A) Holo-*B. japonicum* PBGS. The sample contained 1.8 mL of 113 mg/mL enzyme, 83 mM bis-tris propane at pH 8.2, 8 mM free Mg(II), 83 mM KCl, and 17% (v/v) D_2O. There were 32 000 transients. (B) [3,5-^{13}C]Porphobilinogen bound to *B. japonicum* PBGS. Forty microliters of 0.1 M [4-^{13}C]-ALA was added to the previous sample; 39 000 transients were collected. The dotted lines indicate the resonance positions of free [3,5-^{13}C]porphobilinogen. C) [3,5-^{13}C]Porphobilinogen bound to *B. japonicum* PBGS with Mn(II) in sites A and C. The sample contained 66 mg/mL *B. japonicum* PBGS, 83 mM bis-tris propane at pH 8.2, 1.9 mM Mn(II), 83 mM KCl, and 0.6 mM [3,5-^{13}C]porphobilinogen; 29 500 transients were collected. (D) Free [3,5-^{13}C]porphobilinogen plus apo-*B. japonicum* PBGS. Four microliters of 1 M EDTA, pH 8.2, was added to the previous sample; 36 000 transients were collected. (E) [3,5-^{13}C]porphobilinogen bound to *E. coli* PBGS. The sample contained 1.8 mL of 117 mg/mL *E. coli* PBGS, 83 mM bis-tris propane at pH 8.0, 1.65 mM [3,5-^{13}C]porphobilinogen, 8.3 μM free Zn(II), 0.83 mM free Mg(II), and 8.3 mM 2-mercaptoethanol.

ALA/subunit, illustrated in Figure 5C, shows marked broadening of both signals from enzyme-bound [3,5-^{13}C]porphobilinogen. Line width analysis suggests a larger broadening on the resonance derived from C_5 than that from C_3. This is consistent with an active site model in which the amino group of porphobilinogen is a ligand to Mn_A (see Figure 1). Spectrum 5D illustrates the effect of the addition of 2 mM EDTA to the sample from spectrum 5C. EDTA has a higher affinity for Mn(II) ($K_d \cong 10^{-14}$ M) than does the enzyme; thus, addition of EDTA regenerates apo-PBGS. The removal of Mn_A results in the release of [3,5-^{13}C]porphobilinogen from the enzyme and regeneration of the signal from "free" porphobilinogen. This also supports our model where porphobilinogen is a ligand to Mn_A. Similar EDTA treatment of *B. japonicum* PBGS containing Mg(II) does not result in product release because the affinity of EDTA for Mg(II) ($K_d \cong 10^{-9}$ M) is not tighter than that of the enzyme (data not shown).

DISCUSSION

The porphobilinogen synthases are metalloenzymes that are often classified as requiring either Zn(II) *or* Mg(II) for activity (*18, 19, 20*). Detailed characterization of bovine PBGS demonstrated that although eight Zn(II) bound per homooctamer, there are two distinct Zn(II) binding sites each at four per octamer referred to as site A and site B (*3*). Characterization of the Zn(II) requiring *E. coli* PBGS revealed that the enzyme bound eight Zn(II) and eight Mg(II) per homooctamer under physiological conditions (*6, 13*). This led us to a general model for all PBGS in which any one octamer has four active sites and could use divalent metal ions for up to three distinct roles, as illustrated in Table 1. The active sites of types I and II PBGS both contain Zn_A, while the active sites of types III and IV PBGS contain Mg_A (*9*). Types II, III, and IV all bind the allosteric Mg_C. In this model, both the C_4 oxygen and C_5 amino group of A-side ALA are coordinated to Me_A in the enzyme−substrate complex and the C_{11} amino group of porphobilinogen, derived from A-side ALA, remains coordinated to Me_A in the enzyme−product complex (*1*).

An alternative model exists where each octamer has eight active sites and uses divalent metal ions for two roles in two kinds of binding sites, referred to as site α and site β; each active site contains one Me_α and one Me_β (*13, 14, 15*). In this alternative model: (1) bovine PBGS is an exception with four active sites which contain four α sites and four β sites per homooctamer and both sites bind Zn(II); (2) *E. coli* PBGS is proposed to contain eight α sites and eight β sites per homooctamer where each site binds either Zn(II) or Mg(II), depending upon the buffer pH; and (3) pea PBGS contains eight α sites and eight β sites per homooctamer where each site binds Mg(II). The alternative model proposes only the C_4 oxygen of A-side ALA as a substrate-derived metal ion ligand (*14*). The following discussion relates the current NMR and EPR studies of *B. japonicum* PBGS with those published for bovine and *E. coli* PBGS, and compares the magnetic resonance results with the predictions of the two alternative models.

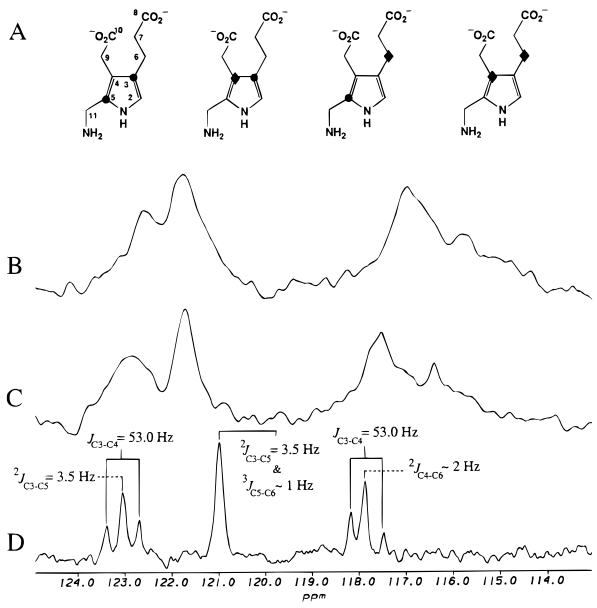

FIGURE 6: ^{13}C NMR of a mixture of ^{13}C -labeled porphobilinogen both free and complexed to *B. japonicum* PBGS. (A) The mixed labeled porphobilinogen was prepared by incubating a 50:50 mix of [4-^{13}C]ALA (●) and [3-^{13}C]ALA (♦) to produce [3,5-^{13}C]-porphobilinogen, [3,4-^{13}C]porphobilinogen, [5,6-^{13}C]porphobilinogen, and [4,6-^{13}C]porphobilinogen in equal amounts. (B) Mixed labeled porphobilinogen bound to *B. japonicum* PBGS. The sample contained 1.8 mL of 104 mg/mL enzyme, 1.35 mM mixed label ALA, 78 mM bis-tris propane, pH 8.2, 8 mM Mg(II), 78 mM KCl, and 22% (v/v) D_2O. The sample was held at 37 °C during the 36 000 transients. (C) Same as (B), except the temperature used was 52 °C. (D) Mixed label porphobilinogen free in solution. The sample contains 2.7 mM porphobilinogen, 78 mM bis-tris propane, pH 8.2, 8 mM Mg(II), 78 mM KCl, a catalytic amount of *B. japonicum* PBGS, and 17% (v/v) D_2O. There were 40 000 transients, and a line broadening of 5 Hz was used to process the data.

The combined EPR and NMR results for *B. japonicum* PBGS presented above are consistent with the predictions of the three divalent cation model for PBGS and cannot be reconciled with the alternative two divalent cation site model of Spencer and Jordan (*13*, *14*, *15*). The evidence for four active sites per octamer is compelling for *B. japonicum* PBGS. The ^{13}C NMR spectra reveal free porphobilinogen upon saturation of four sites per octamer; Mg(II) binding studies reveal four catalytic Mg_A (*9*); and Mn(II) EPR studies are consistent with four Mn_A and inconsistent with eight Mn_A. The NMR evidence also addresses whether *E. coli* PBGS can use a catalytic Mg(II) at certain pH values. Consistent with the model presented in Table 1, a PBGS active site that contains Mg(II) *(B. japonicum)* has a dramatically different chemical environment than those that contain Zn(II) (bovine and *E. coli*), while the latter two are very similar. The near-identity between the ^{13}C NMR spectra of porphobilinogen bound to bovine and *E. coli* PBGS was originally unexpected since the sequence identity is only ~41%. In fact, the overall sequence identity between any pair of these proteins (bovine, *E. coli*, or *B. japonicum*) is only 41−46%. The similarity of the chemical shifts of porphobilinogen bound to bovine or *E. coli* PBGS is now attributed to the close association between Zn_A and porphobilinogen. Porphobilinogen bound to Mg_A has very different chemical shifts. Thus, the NMR data for *E. coli* PBGS with eight Zn(II) and eight Mg(II) over a range of pH values are inconsistent with a model where Zn(II) and Mg(II) are interchangeable in the catalytic site. The collected data on *B. japonicum* PBGS also address the issue of direct ligation of Me_A to substrate or product. We previously showed that at Mg(II) concentrations below the K_d for Mg_A, the K_m for ALA goes above 1 M (*9*). In the absence of substrate or product, Mn(II) primarily binds to the allosteric Me_C site with a stoichiometry of eight per octamer. In the presence of substrate or product, a catalytically essential site is filled first with a stoichiometry of four per octamer, one per active site. We interpret this as evidence for direct ligation between Me_A and both substrate and product. Here we confirm that the addition of porphobilinogen to *B. japonicum* PBGS with Mn(II) bound in the allosteric site results in the disproportionation of the Mn(II) to the catalytic site. A similar Mn(II) EPR experiment with *E. coli* PBGS, which only binds Mn(II) in the allosteric site, indicated that the addition of porphobilinogen had no effect on the EPR spectrum of Mn_C (in the presence of Zn_A) (*6*). In addition, the observed increase in the line width for [3,5-^{13}C]porphobilinogen bound to Mn(II) containing *B. japonicum* PBGS supports the active site model with porphobilinogen bound to the active site divalent metal ion through a deprotonated amine group.

ACKNOWLEDGMENT

We thank Dr. George D. Markham of this institute for use of the Varian E109 X band spectrometer.

REFERENCES

1. Jaffe, E. K. (1995) *J. Bioenerg. Biomembr. 27*, 169−179.
2. Jaffe, E. K., Volin, M., Myers, C. B., and Abrams, W. R. (1994) *Biochemistry 33*, 11554−11562.
3. Dent, A. J., Beyersmann, D., Block, C., and Hasnain, S. S. (1990) *Biochemistry 29*, 7822−7828.
4. Jaffe, E. K., Abrams, W. R., Kaempfen, K. X., and Harris, K. A. (1992) *Biochemistry 31*, 2113−2123.
5. Mitchell, L. W., and Jaffe, E. K. (1993) *Arch. Biochem. Biophys. 300*, 169−177.
6. Jaffe, E. K., Ali, S., Mitchell, L. W., Taylor, K. M., Volin, M., and Markham, G. D. (1995) *Biochemistry 34*, 244−251.
7. Nandi, D. L., Baker-Cohen, K. F., and Shemin, D. (1968) *J. Biol. Chem. 243*, 1224−1230.
8. Nandi, D. K., and Shemin, D. (1968) *J. Biol. Chem. 243*, 1231−1235.
9. Petrovich, R. M., Litwin, A., and Jaffe, E. K. (1996) *J. Biol. Chem. 271*, 8692−8699.
10. Jaffe, E. K., and Markham, G. D. (1987) *Biochemistry 26*, 4258−4264.
11. Jaffe, E. K., and Markham, G. D. (1988) *Biochemistry 27*, 4475−4481.
12. Jaffe, E. K., Markham, G. D., and Rajagopalan, J. (1990) *Biochemistry 29*, 8345−8350.
13. Spencer, P., and Jordan, P. M. (1993) *Biochem. J. 290*, 279−287.
14. Spencer, P., and Jordan, P. M. (1994) *Biochem. J. 300*, 373−381.
15. Spencer, P., and Jordan, P. M. (1995) *Biochem. J. 305*, 151−158.
16. Cohn, M., and Townsend, J. (1954) *Nature 173*, 1090.
17. Chauhan, S., and O'Brian, M. R. (1993) *J. Bacteriol. 175*, 7222−7227.
18. Boese, Q. F., Spano, A. J., Li, J. M., and Timko, M. P. (1991) *J. Biol. Chem. 266*, 17060−17066.
19. Jones, M. C., Jenkins, J. M., Smith, A. G., and Howe, C. J. (1994) *Plant Mol. Biol. 24*, 435−448.
20. Chauhan, S., and O'Brian, M. R. (1995) *J. Biol. Chem. 270*, 19823−19827.
21. Jaffe, E. K. (1993) *Comments Inorg. Chem. 15*, 67−93.
22. Cheung, K., Spencer, P., Timko, M. P., and Shoolingin-Jordan, P. R. (1997) *Biochemistry 36*, 1148−1156.

BI971642A